HHS Public Access

Author manuscript

J Immunol. Author manuscript; available in PMC 2020 March 15.

Published in final edited form as:

J Immunol. 2019 March 15; 202(6): 1747–1754. doi:10.4049/jimmunol.1801569.

L-arginine synthesis from L-citrulline in myeloid cells drives host defense against mycobacteria *in vivo*

Shannon M. Lange[#1,2], **Melanie C. McKell**[#1,2], **Stephanie M. Schmidt**[1], **Junfang Zhao**[3], **Rebecca R. Crowther**[1,2,4], **Lisa C. Green**[1,5], **Rebecca L. Bricker**[1], **Eusondia Arnett**[6], **S. Eleonore Köhler**[7], **Larry S. Schlesinger**[6], **Kenneth D. R. Setchell**[3], and **Joseph E. Qualls**[1,*]

[1]Department of Pediatrics, University of Cincinnati College of Medicine; Division of Infectious Diseases, Cincinnati Children's Hospital Medical Center. [2]Immunology Graduate Program, University of Cincinnati. [3]Department of Pediatrics, Division of Pathology and Laboratory Medicine, Mass Spectrometry Core, Cincinnati Children's Hospital Medical Center. [4]Medical Scientist Training Program, University of Cincinnati. [5]Molecular, Cellular, and Biochemical Pharmacology Graduate Program, University of Cincinnati. [6]Texas Biomedical Research Institute, Maastricht University, Maastricht, Netherlands. [7]Department of Anatomy & Embryology, Maastricht University, Maastricht, Netherlands.

[#] These authors contributed equally to this work.

Abstract

Immunonutrition as a therapeutic approach is rapidly gaining interest in the fight against infection. Targeting L-arginine metabolism is intriguing, considering this amino acid is the substrate for antimicrobial nitric oxide production by macrophages. The importance of L-arginine during infection is supported by the finding that inhibiting its synthesis from its precursor L-citrulline blunts host defense. During the first few weeks following pulmonary mycobacterial infection, we found a drastic increase in L-citrulline in the lung, even though serum concentrations were unaltered. This correlated with increased gene expression of the L-citrulline-generating (i.e. iNOS) and L-citrulline-utilizing (i.e. Ass1) enzymes in key myeloid populations. Eliminating L-arginine synthesis from L-citrulline in myeloid cells via conditional deletion of either *Ass1* or *Asl* resulted in increased *Mycobacterium bovis* BCG and *M. tuberculosis* $H_{37}R_v$ burden in the lungs compared to controls. Our data illustrate the necessity of L-citrulline metabolism for myeloid defense against mycobacterial infection and highlight the potential for host-directed therapy against mycobacterial disease targeting this nutrient and/or its metabolic pathway.

[*]Correspondence: Joseph E. Qualls, Department of Pediatrics, Division of Infectious Diseases, MLC 7017, Cincinnati Children's Hospital Medical Center, 3333 Burnet Ave, Cincinnati, OH 45229. joseph.qualls@cchmc.org. 513-636-9102 (Telephone), 513-636-7039 (Fax).

Author Contributions

Conceptualization, S.M.L., J.E.Q. and M.C.M.; Methodology, all authors; Investigation, S.M.L., J.Z., M.C.M., S.M.S., L.C.G., J.E.Q. and R.R.C., Resources, E.A, L.S.S, S.E.K., K.D.R.S., J.E.Q.; Writing – Original Draft, S.M.L., J.E.Q. and M.C.M.; Writing – Review & Editing, all authors; Supervision, L.S.S., K.D.R.S., J.E.Q.; Funding Acquisition, J.E.Q.

Declaration of Interests

The authors declare no competing interests.

Introduction

Mycobacterium tuberculosis exemplifies a pathogen whose global reach and increasing resistance to pharmacologic interventions heightens the need for novel and more efficient treatment options (1). Host-directed interventions show promise in theory, yet protective correlates and regulatory mechanisms governing the persistence of *M. tuberculosis* in patients and experimental animal models need to be elucidated. Compared to healthy individuals, patients with active tuberculosis (TB) have increased peripheral blood cell arginase activity and reduced systemic L-arginine (L-ARG) (2) – an amino acid necessary for multiple immune functions, including microbicidal nitric oxide (NO) production and robust T cell activity (3). These data correlate with an increase in arginase expression within, and surrounding lung granulomas observed from TB biopsies (4–6). Arginase 1 (Arg1), which metabolizes L-ARG to urea and L-ornithine (L-ORN), is expressed in macrophages following mycobacterial infection, thus limiting L-ARG-dependent anti-mycobacterial defenses (7, 8). As such, L-ARG supplementation, aimed at enhancing immunity against *M. tuberculosis*, has been attempted in TB patients. Yet, despite the importance of L-ARG, its supplementation is largely ineffective at boosting systemic L-ARG levels (9–12) and providing beneficial clinical outcomes (13–16).

Anti-mycobacterial NO production and T cell activity can be fueled by a related amino acid, L-citrulline (L-CIT) (17–20). L-CIT can be acquired from the diet or during metabolic processing of L-ARG (via NO synthases) or L-ORN (via ornithine carbamoyl transferase) (21). Also, it can be used to synthesize L-ARG, entailing the sequential activity of two cytosolic enzymes: argininosuccinate synthase (Ass1) and argininosuccinate lyase (Asl) (21). We have recently uncovered an immune-protective role of this pathway during infection with *M. tuberculosis* and *M. bovis* BCG, in which L-ARG synthesized from L-CIT bypasses arginase-mediated inhibition of NO production and benefits host defense against mycobacterial infection (19, 20).

In the present work, we demonstrate that over the course of *M. bovis* BCG infection, pulmonary L-CIT concentrations rise concurrently with increased iNOS, Ass1, and Asl gene expression in inflammatory macrophages. Utilizing innovative mouse models to selectively delete L-ARG synthesis from L-CIT in myeloid cells, we found diminished clearance of *M. bovis* BCG from the lungs of L-ARG synthesis-deficient mice compared to controls. Lastly, when challenging mice that are unable to synthesize L-ARG in myeloid cells with virulent *M. tuberculosis*, we found increased mycobacterial burden in the lungs, as well as in macrophages from these mice infected *in vitro*. These data suggest L-CIT and the L-CIT/L-ARG metabolism pathways in myeloid cells to be integral to anti-mycobacterial host defense, and targeting these metabolites may prove promising as novel host-directed therapies.

Materials and Methods

Mice.

C57BL/6, *Asl*$^{flox/flox}$;*Lyz2*$^{cre/cre}$, *Asl*$^{flox/flox}$;CD11c-cre, *Asl*$^{flox/flox}$;Tie2-cre, and *Ass1*$^{flox/flox}$;Tie2-cre mice (and cre-negative controls) were bred within the Division of

Veterinary Services at Cincinnati Children's Hospital Medical Center (CCHMC). Strains were originally obtained from The Jackson Laboratories: C57BL/6J, 000664; B6.129S7-*Asl*^{tm1Brle}/J, 018830; B6.129P2-*Lyz2*$^{tm1(cre)Ifo}$/J, 004781; C57BL/6J-Tg(Itgax-cre,-EGFP)4097Ach/J, 007567; B6.Cg-Tg(Tek-cre)1Ywa/J, 008863). *Ass1*$^{flox/flox}$;Tie2-cre mice were a gift from S. E. Kohler (22). Mice for *M. tuberculosis* infections were transferred to the Laboratory Animal Medical Services ABSL3 facility at the University of Cincinnati (UC) one week prior to inoculation. All procedures were approved by the IACUC at CCHMC and UC.

Mycobacterium bovis BCG *in vivo* infection.

M. bovis bacillus Calmette-Guérin (*M. bovis* BCG) Pasteur strain was cultured in 7H9 media (Sigma) plus OADC (Fisher) containing 0.05% Tween-80 (Sigma) at 37°C, shaking at ~50 r.p.m. *M. bovis* BCG bacilli were washed twice with sterile PBS and passed through a 40 μm nylon mesh strainer prior to use. *M. bovis* BCG concentration was determined by measuring absorbance at A_{600} and adjusted to appropriate concentrations in sterile PBS. Mice were anesthetized with isoflurane, and *M. bovis* BCG was administered via intranasal inoculation in 50 μL containing ~1.0 to 5.0 × 10^6 bacilli. Blood was collected from euthanized mice, and lungs and spleens were removed, weighed, and homogenized in sterile PBS. Homogenate dilutions were plated on 7H10 agar (Becton Dickinson) containing OADC and antimicrobials: polymyxin B sulfate (26 μg/mL, Sigma), trimethoprim lactate (20 μg/mL, Sigma), carbenicillin disodium (50 μg/mL, Sigma), and amphotericin B (2.5 μg/mL, Sigma). Plates were incubated at 37°C for 14–21 days prior to counting. Colony forming units (CFU) from the left lung, or spleen (spleen CFU were determine per gram of tissue as half of the spleen was used for additional assays) were determined. For histology, alternate lobes of the lungs were inflated with 10% formalin and processed for H & E staining.

Mycobacterium tuberculosis in vivo infection.

M. tuberculosis $H_{37}R_v$ (luciferase expressing (23)) was cultured in 7H9 media plus OADC containing 0.05% Tween-80 at 37°C shaking ~50 r.p.m. *M. tuberculosis* was prepared and used to infect mice similar to *M. bovis* BCG infection described above. Mice were infected by an intranasal inoculation of 50 μL containing ~0.1 to 1.0 × 10^2 bacilli, as confirmed by plating on 7H11 agar (Sigma). Eight weeks following infection, lungs and spleens were removed from euthanized mice and homogenized in sterile PBS. Serial dilutions of the homogenate were plated on 7H11 agar containing OADC and antimicrobial cocktail described above for 7H10 agar plates. Agar plates were incubated at 37°C for >21 days prior to counting colonies. Viable *M. tuberculosis* bacilli were determined as colony forming units (CFU) from the left lung or spleen.

Tissue culture and *M. tuberculosis in vitro* infection.

Media: Complete Dulbecco's Modified Eagles Media (C-DMEM, 10–013-CV, Cellgro, Corning Life Sciences) was prepared by adding bovine calf serum (SH30073.03, Thermo Fisher Scientific) to 10%, and penicillin / streptomycin (15140–122, Gibco, Life Technologies) to 1% final concentration. L-arginine-free C-DMEM lacking phenol red (D9443 Sigma) was prepared by adding dialyzed fetal bovine serum (35–071-CV, Cellgro,

Corning Life Sciences) to 10% final concentration plus L-glutamine (25030–081, Life Technologies), L-lysine-HCl (L8662, Sigma), L-leucine (L8912, Sigma), sodium pyruvate (11360–070, Life Technologies), and D-glucose (G8796, Sigma) to concentrations found in C-DMEM. L-arginine (A8094, Sigma) and L-citrulline (C7629, Sigma) were prepared at a stock concentration of 100 mM in sterile water. L-arginine and L-citrulline stocks were added to L-arginine-free C-DMEM to concentrations noted in the text. Peritoneal-derived MΦs (PDMs): Mice were administered 1 ml sterile thioglycollate (R064710, Fischer Scientific) by intraperitoneal injection. After 4 days, peritoneal cells were collected by lavage. Following red cell lysis, cells were plated at 2×10^5 per well on a white 96-well tissue culture plate (353296, Fisher Scientific) in C-DMEM. C-DMEM and non-adherent cells were aspirated after overnight incubation, and fresh L-arginine-free C-DMEM was added with L-arginine and/or L-citrulline. *M. tuberculosis* $H_{37}R_v$ was prepared as above, and adjusted to co-culture with macrophages at a MOI = 0.1. After 72 hours, mycobacterial viability was determined by analyzing relative luminescence units (RLUs) using a DTX-880 Mutltimode plate reader and detection software (Beckman Coulter). Nitric oxide production was determined by measuring NO_2^- by Griess assay.

Griess Assay.

Equal volumes of cell culture supernatant and Griess reagent (0.5 g sulfanilamide (S9251, Sigma), 0.05 g N-(1-Naphthyl)ethylenediamine dihydrochloride (33461, Sigma), and 1.17 mL phosphoric acid per 50 mL water) were mixed in a 96 well plate. Sodium nitrite (237213, Sigma) was used as a standard. Absorbance values were measured immediately at A_{492} using a DTX-880 Mutltimode plate reader and detection software (Beckman Coulter).

Liquid chromatography tandem mass spectrometry (LC-MS/MS).

Amino acid analytes were extracted from serum and lung homogenate samples by protein precipitation followed by centrifugation. The stable-isotope labeled amino acids were added to the precipitation reagent and used as the internal standards. Amino acid analytes were determined and measured by LC-MS/MS with multiple reaction monitoring (MRM). All samples were analyzed with the LC20AD HPLC system (Shimadzu) coupled to the SCIEX QTRAP 5500 mass spectrometer (Sciex, Concord, Canada). Chromatographic separation of amino acid analytes was achieved on a 100 × 2.1 mm Atlantis HILIC column (Waters). A gradient mobile phase was used with a binary solvent system, which changed from 80% mobile phase B (95% acetonitrile/5% water/0.1% formic acid/1.5 mM ammonium formate) to 35% mobile phase A (water/0.1% formic acid/1.5 mM ammonium formate) at a flow rate of 0.5 mL/minute. The total run time was 8 minutes. The optimal signal for the analytes were achieved in positive ion mode with the use of the following instrument settings: Ionspray voltage (IS): 5000v; Source temperature (TEM): 550°C; Curtain Gas (CUR): 35 psi; Ion source gas 1 (GS1): 60 psi and Ion source gas 2 (GS2): 50 psi. Data acquisition on the mass spectrometer was controlled by Analyst 1.6.2 software (Sciex, Concord, Canada). Data processing and quantification were performed with MultiQuant software version 3.0 (Sciex, Concord, Canada).

RNA analysis.

Lungs from euthanized mice were removed, minced, and digested in C-DMEM supplemented with 1 mg/ml collagenase (C7657, Sigma) and 0.5 mg/ml deoxyribonuclease I (LS002139, Worthington Biochemical) for 1 hour at 37°C. Lung digests were processed into a single cell suspension, were blocked with 5% normal mouse serum and prepared for magnetic sorting with anti-CD11c beads (130–052-001, Miltenyi BioTec), followed by anti-CD11b beads (130–049-601, Miltenyi BioTec) in indicated samples. In some experiments, lung digests were subjected to fluorescence activated cell sorting (FACS) using antibodies against CD11b (clone M1/70. Invitrogen), CD11c (clone N418, eBiosciences), CD45 (clone 104, Invitrogen), and a live/dead stain (65–0865-14, Invitrogen). Sorted cells were lysed in Trizol (Fisher Scientific) for RNA analysis and prepared for RNA purification following the manufacturer's protocol. RNA was converted to cDNA using SuperScript II reverse transcriptase (Invitrogen) with a mixture of oligo dT and random primers (Invitrogen). cDNA was analyzed by SybrGreen qRT-PCR (Applied Biosystems). Primers: iNOS (F: 5` AGCTCCACAAGCTGGCTCGCTTT 3`, R: 5` TTGTTGCTGAACTTCCAGTCAT 3`; Ass1 (F: 5` CTCGCAGACAGGTGGAGATT 3`, R: 5` GCCAGTGAATAGCAGGTGAG 3`); Asl (F: 5` ACTCTTGGAGGTGCAGAAGC 3`, R: 5` AGTAGCTCCCGGTCCACAC 3`); Arg1 (F: 5` TCGAGGAGGGGTAGAGAAAG 3`, R: 5` GACATCAACAAAGGCCAGGT 3`), Arg2 (F: 5` GTGTCACCATGGGAGGAGACCA 3`, R: 5` TAATGTCCGCATGAGCATCAACC 3`), Gapdh (F: 5` GGTGCTGAGTATGTCGTGGA 3`, R: 5` CGGAGATGATGACCCTTTTG 3`).

Statistics.

Error bars represent the standard deviation (SD). Box and whisker plots display the interquartile (box) and maximal (whisker) range of data stemming from the median (line). Data were analyzed for statistical significance by Student's t test or 2-way ANOVA as appropriate. Indicators of statistical significance and the test utilized are found within the figure legends.

Results

L-CIT fluctuation during mycobacterial infection

Amino acid availability and regulation during mycobacterial disease have been largely recognized in the context of L-ARG metabolism by opposing enzymatic pathways in myeloid cells: iNOS and Arg1 (3). Low plasma L-ARG correlates with elevated arginase activity in TB patients as compared to healthy controls (2). Concentrations of amino acids in infected lungs, however, have not been investigated. We first sought to establish how attenuated mycobacterial infection impacted relevant amino acid concentrations (Fig 1A). Following intranasal *M. bovis* BCG inoculation, mycobacterial burden steadily declined 2 weeks post-infection, and remained low after 16 weeks (Fig. 1B). Quantification of L-ARG, L-CIT, and L-ORN in the serum revealed no significant changes compared to uninfected (i.e. week 0) controls (Fig 1C). Relative amounts of these amino acids at the site of infection, however, were quite different from those in systemic circulation. Lung L-ARG and L-ORN increased moderately over the course of infection, whereas L-CIT concentrations sharply increased > 4.5-fold by 6 weeks post-infection (Fig 1D). L-CIT decreased between 6 and 16

weeks post-infection, yet its concentration at 16 weeks was still elevated relative to uninfected mice.

These data demonstrate differences between systemic and lung amino acids throughout infection. Further investigation and development of techniques to differentiate between intracellular and extracellular amino acids will be necessary to determine availability, localization, and transport of amino acids and other metabolites within the infected lung. Nevertheless, these analyses show dramatic fluctuation in L-CIT, leading us to question which cells involved in host defense might be responsible for the production and utilization of this amino acid.

Lung myeloid populations increase gene expression of L-CIT generating and utilizing enzymes

Tissue-resident alveolar macrophages and recruited macrophages within the lung harbor mycobacteria and have been observed to express iNOS (24, 25), yet less is known about L-CIT metabolism within these cells. To investigate this, we quantified iNOS, Ass1, and Asl expression in myeloid populations from *M. bovis* BCG-infected lungs at 2, 6, and 16 weeks post-infection (Fig 2A). Cells were magnetically sorted based on integrin expression: $CD11c^{+}$ – predominantly alveolar macrophages, dendritic cells (DCs), and other macrophage populations; $CD11c^{neg}CD11b^{+}$ – recruited monocytes, neutrophils and other granulocytes; $CD11c^{neg}CD11b^{neg}$ – non-myeloid cells (Fig 2A, B). When analyzing gene expression from these populations, we found iNOS and Ass1 were induced in $CD11c^{+}$ and $CD11c^{neg}CD11b^{+}$ cells (Fig 2C). Both iNOS and Ass1 were increased in $CD11c^{+}$ cells relative to $CD11c^{neg}CD11b^{+}$ cells, suggesting a greater role of L-ARG synthesis in this population. Asl remained constant in all populations, consistent with descriptions of Ass1 as the rate-limiting step of L-ARG synthesis from L-CIT (26).

In order to confirm our findings from the magnetically sorted lung cells, and to further separate the $CD11c^{+}$ population into $CD11b^{+}$ and $CD11b^{neg}$ populations, we next turned to fluorescence activated cell sorting (FACS). Mice were infected with *M. bovis* BCG, and lungs were digested as in Fig 2A. Lung cells were sorted from uninfected mice, and 2 and 6 weeks post *M. bovis* BCG infection (Fig 2D). Relative frequencies of the myeloid cells with different CD11c and CD11b expression were determined from $CD45^{+}$ hematopoietic cells (Fig. 2E). Following gene expression profiling, we confirmed that $CD11c^{+}$ lung cells primarily accounted for increased iNOS and Ass1 gene expression, and these cells also expressed CD11b – previously reported as inflammatory macrophages (27). Interestingly, this population also displayed an increase in Asl following infection, which was significantly higher than that found in $CD11c^{neg}CD11b^{+}$ or $CD11c^{neg}CD11b^{neg}$ cells.

Considering the known role for arginase in mycobacterial infection (4, 7), we analyzed which population(s) of myeloid cells were involved in L-ARG metabolism to urea and L-ORN. While type I arginase (Arg1, cytosolic) was relatively low between 6–16 weeks post infection and was broadly found in $CD11c^{+}$ and $CD11b^{+}$ cells, type II arginase (Arg2, mitochondrial) was mainly found within the $CD11c^{neg}CD11b^{+}$ population, perhaps due to the increased expression of this arginase in neutrophils (Supplemental Fig 1A, B). It is

possible that these cells are responsible for the increase in lung L-ORN found between 6 and 16 weeks post-mycobacterial infection (Fig 1D).

Taken together, our data implicate $CD11c^{+}CD11b^{+}$ inflammatory macrophages as the predominant L-ARG synthesizing cells present in the mycobacteria-infected lung (Fig 2, Supplemental Fig 1). Considering the drastic increase in the frequency of these cells following infection, it is still unclear if these are induced to express iNOS/Ass1/Asl following recruitment, if they are primed prior to lung migration, or a combination of the two. Regardless, myeloid cells doubly expressing the integrins CD11c and CD11b increase gene expression of both L-ARG utilizing and synthesizing enzymes, and we were curious if host defense against mycobacteria required L-ARG synthesis from this cell population.

Myeloid L-ARG synthesis enhances host defense against mycobacterial infection *in vivo*

Our data suggest that L-CIT is metabolized by myeloid cells for L-ARG synthesis during mycobacterial infection. Whether L-ARG synthesis from L-CIT in these cells is necessary for host defense, however, is unknown. We previously observed a requirement for Ass1 in bone marrow-derived cells to limit mycobacterial burden in mouse lungs (19), yet the responsible cell population(s) was not determined. Systemic Ass1 or Asl deletion causes liver dysfunction and hyperammonemia, resulting in early lethality (28–31). Here, we utilized tissue-specific models of Asl and Ass1 deficiency to probe the necessity of L-CIT metabolism for anti-mycobacterial defense in myeloid populations of interest by crossing $Asl^{flox/flox}$ or $Ass1^{flox/flox}$ mice to promoter-driven Cre recombinases (Fig 3A, Supplemental Fig 2A).

$Asl^{flox/flox}$ mice (28) were crossed with Tie2-cre expressing mice to eliminate Asl expression in hematopoietic and endothelial cells. We have previously shown that macrophages from $Asl^{flox/flox}$;Tie2-cre mice are impaired at blocking mycobacteria growth *in vitro* when cultured in L-ARG-free media supplemented with L-CIT (20). These and control mice were infected with *M. bovis* BCG *in vivo*. As expected, Asl was reduced in myeloid populations from $Asl^{flox/flox}$;Tie2-cre mice compared to controls (Fig 3B). Mycobacterial burden in the lung was significantly higher in Tie2-cre-expressing mice compared to controls (Fig 3C), confirming the necessity of Asl in regulating mycobacterial infection.

In order to dissect the contribution of L-CIT metabolism in myeloid cells during mycobacterial infection, $Asl^{flox/flox}$;$Lyz2^{cre/cre}$ and $Asl^{flox/flox}$;CD11c-cre mice were generated (Fig 3A). Asl was reduced in the $CD11c^{+}$ population for both mouse strains, and within the $CD11c^{neg}CD11b^{+}$ population from $Asl^{flox/flox}$;$Lyz2^{cre/cre}$ mice (Fig 3B). Mycobacterial growth from the lungs revealed that both $Asl^{flox/flox}$;$Lyz2^{cre/cre}$ and $Asl^{flox/flox}$;CD11c-cre mice contained more mycobacteria compared to controls (2.5-fold and 2.0-fold, respectively, Fig 3C). Differences in splenic CFUs were less dramatic in each of the $Asl^{flox/flox}$ models (Fig 3D). To exclude a possible role for L-argininosuccinate, the intermediate of L-ARG synthesis from L-CIT, in inhibiting immune function, we crossed $Ass1^{flox/flox}$ (22) with Tie2- and Lyz2-cre expressing mice. *M. bovis* BCG-infected $Ass1^{flox/flox}$;Tie2-cre, and $Ass1^{flox/flox}$;$Lyz2^{cre/cre}$ mice displayed an increase in mycobacterial load in the lung and spleen as compared to controls (Supplemental Fig 2),

suggesting both components of L-ARG synthesis – L-CIT to L-argininosuccinate by Ass1, and L-argininosuccinate to L-ARG by Asl – are integral to host defense. When analyzing lung pathology from *M. bovis* BCG-infected mice, we also observed increased inflammation in mice lacking either Asl or Ass1 in hematopoietic or myeloid lineages as compared to infected controls (Supplemental Fig 3).

L-ARG synthesis from L-CIT in myeloid cells enhances host defense during challenge with virulent *M. tuberculosis* infection *in vitro* and *in vivo*

We next questioned the necessity of myeloid L-ARG synthesis in controlling virulent *M. tuberculosis* infection. Thioglycollate-elicited peritoneal-derived macrophages (PDMs) were collected from either *Asl*$^{flox/flox}$;*Lyz2*$^{cre/cre}$, *Ass1*$^{flox/flox}$;*Lyz2*$^{cre/cre}$, or control WT mice, stimulated with IFN-γ, and infected with virulent *M. tuberculosis* $H_{37}R_v$ containing a luciferase construct, enabling detection of viable mycobacteria by analyzing relative luminescence units (RLUs) across time / stimulation conditions (23, 32). Similar to our previous work, we found that macrophages required either L-CIT or L-ARG to effectively decrease mycobacterial viability (Fig 4A), and this correlated with an increase in NO production (Fig 4B). Eliminating L-ARG synthesis from L-CIT by ablation of either Asl or Ass1 reduced macrophage NO production and mycobacterial control when cultured in either L-ARG or L-CIT (Fig 4A, B). Still, this was most pronounced in culture conditions containing only L-CIT, where macrophages lose nearly all NO production and mycobacterial viability is unaltered compared to when neither L-ARG nor L-CIT are present in culture media (Fig 4A, B, left panels). As such, we conclude that L-ARG synthesis is necessary for optimal control of virulent *M. tuberculosis in vitro*.

We next addressed the necessity of myeloid L-ARG synthesis for host defense against virulent *M. tuberculosis in vivo*. *Asl*$^{flox/flox}$;*Lyz2*$^{cre/cre}$, *Ass1*$^{flox/flox}$;*Lyz2*$^{cre/cre}$, and *Lyz2*$^{cre/cre}$ controls were infected with *M. tuberculosis* $H_{37}R_v$ by intranasal inoculation. Following eight weeks of infection, mice were euthanized and CFUs were determined from the lungs and spleen. In agreement with data obtained during *M. bovis* BCG infection, mice lacking myeloid Asl or Ass1 failed to control *M. tuberculosis* growth in the lung (Fig 4C). Therefore, L-ARG synthesis in macrophages and possibly other myeloid cells is essential for optimal host defense against *M. tuberculosis in vitro* and *in vivo*.

Discussion

We find that inflammatory macrophage (and other myeloid cell) synthesis of L-ARG from L-CIT is activated following mycobacterial infection (Fig 2), and elimination of this pathway in myeloid cells (using myeloid-conditional knockouts of As1 and Ass1) significantly reduces anti-mycobacterial host defense *in vitro* and *in vivo* (Fig 3, 4). Furthermore, eliminating Asl or Ass1 from the myeloid compartment reduced host defense to the same degree as eliminating these enzymes from the entire hematopoietic/endothelial compartment (using Tie2-driven conditional deletion) when analyzing changes in *M. bovis* BCG lung CFUs between these mouse strains (Fig 3, Supplemental Fig. 2). Still, this does not exclude a contribution of L-ARG synthesis in other hematopoietic immune cells (or non-immune cells) during mycobacterial infection. As mentioned, using *Asl*$^{flox/flox}$;Tie2cre mice

will delete *Asl* in endothelial cells, and unfortunately no other "hematopoietic" conditional knockouts are available that are devoid of endothelial involvement (33). Yet if L-ARG synthesis is necessary in other cells, its loss in non-myeloid populations does not alter mycobacterial burden in the lung (i.e. comparing deletion by $Lyz2^{cre/cre}$ to Tie2cre) at the eight week end-point of these studies. Regardless, with the known importance of L-ARG synthesis in endothelial cells (21, 22, 34, 35) and T cells (17, 18, 36–38), further investigation into how L-CIT metabolism affect these and other cell populations during infection warrants investigation. Considering the fluctuation of L-CIT in the lung (Fig 1) and increase in inflammatory macrophages with elevated gene expression for enzymes that synthesize (i.e. iNOS) and utilize (i.e. Ass1) L-CIT (Fig 2), our data reveal an essential role for L-ARG synthesis in myeloid cells during mycobacterial infection.

Focusing on the myeloid compartment, we expect that lung inflammatory macrophages drive L-CIT-mediated host defense. DCs and granulocytes may also contribute considering they also cannot synthesize L-ARG from L-CIT in $Asl^{flox/flox}$;CD11c-cre and $Asl^{flox/flox}$;$Lyz2^{cre/cre}$ (or $Ass1^{flox/flox}$;$Lyz2^{cre/cre}$) mice, respectively. Infected pulmonary DCs are vital for $CD4^+$ and $CD8^+$ T cell activation and recruitment to the lung (39). Their metabolic programming, however, is not yet understood. We are currently addressing the contribution of L-ARG synthesis in DCs, especially in the context of initiating the adaptive response via interactions with naïve T cells. Additionally, whether L-CIT is converted to L-ARG in neutrophils has yet to be investigated. Human neutrophils and granulocytic myeloid-derived suppressor cells are known to constitutively express and secrete arginase (40) and may function as additional mediators of L-ARG sequestration. Hematopoietic-derived adaptive immune cells may also require L-ARG synthesis during infection. Yet, eliminating L-ARG synthesis solely in $CD4^+$ and $CD8^+$ T cells (using CD4-cre conditional knockouts) does not alter mycobacterial burden (18). Collectively, these data show that L-CIT metabolism is necessary within myeloid cells to drive host defense against mycobacterial infection.

We anticipate that active research into metabolic pathways involved during infectious disease and other pathologies will greatly expand our understanding of cellular interactions within distinct tissues. Our data in Figure 1, showing significant increases in amino acids in the lung without substantial changes in serum (Fig 1C, D), highlight the fact that relying solely on systemic metabolic panels is not sufficient to fully appreciate cellular metabolism within specific tissue microenvironments, such as the lung during pulmonary mycobacterial infection. However, our data leave several aspects of metabolism within these tissue microenvironments to be explored. For example, our data examine amino acid changes within the whole tissue at a given time point and do not provide an insight into the specific localization and availability of these amino acids within the infectious microenvironment. To address questions such as these, a combination of metabolic analyses is necessary. The study of metabolic flux within tissue microenvironments can be addressed using technology including matrix-assisted laser desorption and ionization-mass spectrometry imaging (MALDI-MSI), where histology sections can be examined for metabolite availability and overlaid with immunohistochemical staining to understand the localization of these metabolites to sites of pathology. One study, by Marakalala et al., used mass spectrometry analysis to profile human *M. tuberculosis* granuloma sections for differentially distributed

proteins followed by proteome analysis and MALDI-MSI to identify inflammatory markers in distinct regions of granulomas (41). Further, the use of targeted approaches, including those visualizing inflammatory nodules in experimental mycobacterial infections, can provide insight into the metabolic flux within tissue microenvironments. For example, by using a fluorescent glucose analog, such as 2-deoxy-2-[^{18} F]-fluoro-D glucose (FDG), paired with positron emission tomography (PET), glucose utilization within tissue microenvironments can be determined (42). In addition, FDG and PET have been used to identify active granulomas and track treatment efficacy in TB patients (43–45). In the context of L-ARG and L-CIT metabolism, these technologies can be used to understand where these amino acids are localizing within an infected tissue and what metabolic substrates are utilized in tandem with L-ARG and L-CIT. When combined with techniques to understand metabolite utilization, such as transcriptomics, epigenomics, and proteomics approaches, a more complete picture can be obtained of how cellular metabolism occurs during infection and how it impacts distinct pathologies.

Clearly the loss of L-ARG synthesis results in decreased host defense to mycobacterial infection. However, whether L-ARG synthesis can be targeted to enhance host defense has yet to be determined. We are currently addressing how supplementing mice with L-CIT increases host defense as our preliminary data show decreased lung *M. bovis* BCG CFUs in mice treated with L-CIT compared to similarly infected controls (data not shown). Previous work supplementing TB patients with L-ARG has been variable, but largely unsuccessful, potentially due in part to low bioavailability (13–16, 46, 47). L-CIT supplementation, on the other hand, has been observed to augment circulating L-CIT and L-ARG in mouse and human subjects (9, 48). Although the involvement of L-ARG synthesis in TB patients is unknown, ASS1 is induced in human macrophages following inflammatory stimuli (49), suggesting L-ARG synthesis may be involved during immune/inflammatory responses in higher mammals. Furthermore, deterioration of individuals suffering from urea cycle deficiencies (including ASS1 and ASL deficiencies) is commonly associated with infection (50, 51), implying roles for these enzymes in host defense as well as nitrogen elimination. Therefore, we hypothesize that L-CIT supplementation may boost host defense to mycobacterial infection, and we are actively investigating the mechanisms involved during supplementation. Still, why supplement with L-CIT when the end product of L-ARG is the goal? Despite L-ARG's potential as an immune-promoting agent (e.g. substrate for NO production), exogenous L-ARG may prove ineffective due to its low bioavailability. Oral L-ARG is predominantly removed from circulation by hepatocytes (47, 52). Additionally, arginase activity in circulating peripheral blood cells – which is increased in TB patients – may further decrease systemic L-ARG in human disease (2). Arg1-expressing macrophages and granulocytes at the site of infection may deplete the extracellular milieu of L-ARG (5). And unfortunately, L-ARG doses large enough to consistently increase circulating L-ARG levels cause adverse gastrointestinal side effects (46, 53), eliminating it as an ideal long-term nutritional supplement. Conversely, L-CIT is safe, better tolerated in humans, and already in use to treat other disorders (11, 12, 47, 54, 55). We have previously demonstrated that it provides an advantage to iNOS-mediated defense in macrophages by bypassing downstream metabolism by Arg1 (20). Here, we suggest L-CIT as an adjunctive to augment current TB therapies. TB treatment currently relies on extensive combinations of antibiotics, however

many of these chemotherapies function only when the bacteria are metabolically active (56). Enhancement of immune function via L-CIT supplementation in conjunction with antibiotic treatment may provide the host with a faster, stronger response to assist in mycobacterial eradication. Future studies analyzing suitable L-CIT dosing and the efficacy of L-CIT supplementation for the treatment of *M. tuberculosis* with and without antibiotic intervention will provide additional insight into how nutritional supplementation might translate as a therapy to treat TB.

In conclusion, we find that mycobacterial infection induces a significant increase in lung L-CIT, and L-ARG synthesis from L-CIT by myeloid cells is necessary to combat mycobacteria infection *in vitro* and *in vivo*. Furthermore, we expect targeting this pathway by L-CIT supplementation or other targeted approaches to increase L-ARG synthesis will enhance mycobacterial control. Additionally, future studies should consider targeting L-ARG synthesis to enhance host defense to virulent mycobacterial challenge as well as potentially augmenting vaccination strategies. If these experiments prove successful, they will strengthen L-CIT as a potential nutritional therapy to reduce the burden of *M. tuberculosis* in patient populations.

Supplementary Material

Refer to Web version on PubMed Central for supplementary material.

Acknowledgements

We thank Drs. E. Janssen, C. Chougnet, G. Deepe, J. Aliberti, S.S. Way, D. Haslam, T. Alenghat, and H. Deshmukh, as well as members of their laboratories, for invaluable discussions during manuscript preparation. All flow cytometric data were acquired using equipment maintained by the Research Flow Cytometry Core in the Division of Rheumatology at CCHMC

This work was supported by the American Heart Association Scientist Development Grant 15SDG21550007 (JEQ), the National Institutes of Health R01AI116668 (JEQ), the American Association of Immunologists Careers in Immunology Fellowship (JEQ, SML), a Research Innovation and Pilot Award from Cincinnati Children's Hospital Medical Center (JEQ), and the Division of Infectious Diseases at Cincinnati Children's Hospital Medical Center.

References

1. WHO. 2017 Global Tuberculosis Report 2017. World Health Organization: p. http://www.who.int/tb/publications/global_report/en/.
2. Zea AH, Culotta KS, Ali J, Mason C, Park HJ, Zabaleta J, Garcia LF, and Ochoa AC 2006 Decreased expression of CD3zeta and nuclear transcription factor kappa B in patients with pulmonary tuberculosis: potential mechanisms and reversibility with treatment. J Infect Dis. 194(10): p. 1385–93. DOI: 10.1086/508200. [PubMed: 17054067]
3. Rodriguez PC, Ochoa AC, and Al-Khami AA 2017 Arginine Metabolism in Myeloid Cells Shapes Innate and Adaptive Immunity. Front Immunol. 8: p. 93 DOI: 10.3389/fimmu.2017.00093. PMCID: PMC5293781. [PubMed: 28223985]
4. Duque-Correa MA, Kuhl AA, Rodriguez PC, Zedler U, Schommer-Leitner S, Rao M, Weiner J, 3rd, Hurwitz R, Qualls JE, Kosmiadi GA, Murray PJ, Kaufmann SH, and Reece ST 2014 Macrophage arginase-1 controls bacterial growth and pathology in hypoxic tuberculosis granulomas. Proc Natl Acad Sci U S A. 111(38): p. E4024–32. DOI: 10.1073/pnas.1408839111. PMCID: PMC4183271. [PubMed: 25201986]
5. Mattila JT, Ojo OO, Kepka-Lenhart D, Marino S, Kim JH, Eum SY, Via LE, Barry CE, 3rd, Klein E, Kirschner DE, Morris SM, Jr., Lin PL, and Flynn JL 2013 Microenvironments in tuberculous

granulomas are delineated by distinct populations of macrophage subsets and expression of nitric oxide synthase and arginase isoforms. J Immunol. 191(2): p. 773–84. DOI: 10.4049/jimmunol.1300113. PMCID: PMC3746594. [PubMed: 23749634]

6. Pessanha AP, Martins RA, Mattos-Guaraldi AL, Vianna A, and Moreira LO 2012 Arginase-1 expression in granulomas of tuberculosis patients. FEMS Immunol Med Microbiol. 66(2): p. 265–8. DOI: 10.1111/j.1574-695X.2012.01012.x. [PubMed: 22827286]
7. El Kasmi KC, Qualls JE, Pesce JT, Smith AM, Thompson RW, Henao-Tamayo M, Basaraba RJ, Konig T, Schleicher U, Koo MS, Kaplan G, Fitzgerald KA, Tuomanen EI, Orme IM, Kanneganti TD, Bogdan C, Wynn TA, and Murray PJ 2008 Toll-like receptor-induced arginase 1 in macrophages thwarts effective immunity against intracellular pathogens. Nat Immunol. 9(12): p. 1399–406. DOI: 10.1038/ni.1671. PMCID: PMC2584974. [PubMed: 18978793]
8. Qualls JE, Neale G, Smith AM, Koo MS, DeFreitas AA, Zhang H, Kaplan G, Watowich SS, and Murray PJ 2010 Arginine usage in mycobacteria-infected macrophages depends on autocrine-paracrine cytokine signaling. Sci Signal. 3(135): p. ra62 DOI: 10.1126/scisignal.2000955. PMCID: PMC2928148. [PubMed: 20716764]
9. Agarwal U, Didelija IC, Yuan Y, Wang X, and Marini JC 2017 Supplemental Citrulline Is More Efficient Than Arginine in Increasing Systemic Arginine Availability in Mice. J Nutr. 147(4): p. 596–602. DOI: 10.3945/jn.116.240382. PMCID: PMC5368575. [PubMed: 28179487]
10. Wijnands KA, Castermans TM, Hommen MP, Meesters DM, and Poeze M 2015 Arginine and citrulline and the immune response in sepsis. Nutrients. 7(3): p. 1426–63. DOI: 10.3390/nu7031426. PMCID: PMC4377861. [PubMed: 25699985]
11. Wijnands KA, Meesters DM, van Barneveld KW, Visschers RG, Briede JJ, Vandendriessche B, van Eijk HM, Bessems BA, van den Hoven N, von Wintersdorff CJ, Brouckaert P, Bouvy ND, Lamers WH, Cauwels A, and Poeze M 2015 Citrulline Supplementation Improves Organ Perfusion and Arginine Availability under Conditions with Enhanced Arginase Activity. Nutrients. 7(7): p. 5217–38. DOI: 10.3390/nu7075217. PMCID: PMC4516994. [PubMed: 26132994]
12. Wijnands KA, Vink H, Briede JJ, van Faassen EE, Lamers WH, Buurman WA, and Poeze M 2012 Citrulline a more suitable substrate than arginine to restore NO production and the microcirculation during endotoxemia. PLoS One. 7(5): p. e37439 DOI: 10.1371/journal.pone.0037439. PMCID: PMC3362574. [PubMed: 22666356]
13. Farazi A, Shafaat O, Sofian M, and Kahbazi M 2015 Arginine adjunctive therapy in active tuberculosis. Tuberc Res Treat. 2015: p. 205016 DOI: 10.1155/2015/205016. PMCID: PMC4334935. [PubMed: 25734013]
14. Ralph AP, Waramori G, Pontororing GJ, Kenangalem E, Wiguna A, E. Tjitra Sandjaja, Lolong DB, Yeo TW, Chatfield MD, Soemanto RK, Bastian I, Lumb R, Maguire GP, Eisman J, Price RN, Morris PS, Kelly PM, and Anstey NM 2013 L-arginine and vitamin D adjunctive therapies in pulmonary tuberculosis: a randomised, double-blind, placebo-controlled trial. PLoS One. 8(8): p. e70032 DOI: 10.1371/journal.pone.0070032. PMCID: PMC3743888. [PubMed: 23967066]
15. Schon T, Elias D, Moges F, Melese E, Tessema T, Stendahl O, Britton S, and Sundqvist T 2003 Arginine as an adjuvant to chemotherapy improves clinical outcome in active tuberculosis. Eur Respir J. 21(3): p. 483–8. [PubMed: 12662006]
16. Schon T, Idh J, Westman A, Elias D, Abate E, Diro E, Moges F, Kassu A, Ayele B, Forslund T, Getachew A, Britton S, Stendahl O, and Sundqvist T 2011 Effects of a food supplement rich in arginine in patients with smear positive pulmonary tuberculosis--a randomised trial. Tuberculosis (Edinb). 91(5): p. 370–7. DOI: 10.1016/j.tube.2011.06.002. [PubMed: 21813328]
17. Bansal V, Rodriguez P, Wu G, Eichler DC, Zabaleta J, Taheri F, and Ochoa JB 2004 Citrulline can preserve proliferation and prevent the loss of CD3 zeta chain under conditions of low arginine. JPEN J Parenter Enteral Nutr. 28(6): p. 423–30. [PubMed: 15568289]
18. Lange SM, McKell MC, Schmidt SM, Hossfeld AP, Chaturvedi V, Kinder JM, McAlees JW, Lewkowich IP, Way SS, Turner J, and Qualls JE 2017 l-Citrulline Metabolism in Mice Augments CD4+ T Cell Proliferation and Cytokine Production In Vitro, and Accumulation in the Mycobacteria-Infected Lung. Frontiers in Immunology. 8(1561). DOI: 10.3389/fimmu.2017.01561.
19. Qualls JE, Subramanian C, Rafi W, Smith AM, Balouzian L, DeFreitas AA, Shirey KA, Reutterer B, Kernbauer E, Stockinger S, Decker T, Miyairi I, Vogel SN, Salgame P, Rock CO, and Murray

PJ 2012 Sustained generation of nitric oxide and control of mycobacterial infection requires argininosuccinate synthase 1. Cell Host Microbe. 12(3): p. 313–23. DOI: 10.1016/j.chom.2012.07.012. PMCID: PMC3444824. [PubMed: 22980328]

20. Rapovy SM, Zhao J, Bricker RL, Schmidt SM, Setchell KD, and Qualls JE 2015 Differential Requirements for L-Citrulline and L-Arginine during Antimycobacterial Macrophage Activity. J Immunol. 195(7): p. 3293–300. DOI: 10.4049/jimmunol.1500800. [PubMed: 26311904]
21. Curis E, Nicolis I, Moinard C, Osowska S, Zerrouk N, Benazeth S, and Cynober L 2005 Almost all about citrulline in mammals. Amino Acids. 29(3): p. 177–205. DOI: 10.1007/s00726-005-0235-4. [PubMed: 16082501]
22. Marion V, Sankaranarayanan S, de Theije C, van Dijk P, Hakvoort TB, Lamers WH, and Kohler ES 2013 Hepatic adaptation compensates inactivation of intestinal arginine biosynthesis in suckling mice. PLoS One. 8(6): p. e67021 DOI: 10.1371/journal.pone.0067021. PMCID: PMC3681768. [PubMed: 23785515]
23. Salunke SB, Azad AK, Kapuriya NP, Balada-Llasat JM, Pancholi P, Schlesinger LS, and Chen CS 2015 Design and synthesis of novel anti-tuberculosis agents from the celecoxib pharmacophore. Bioorg Med Chem. 23(9): p. 1935–43. DOI: 10.1016/j.bmc.2015.03.041. [PubMed: 25818768]
24. Nozaki Y, Hasegawa Y, Ichiyama S, Nakashima I, and Shimokata K 1997 Mechanism of nitric oxide-dependent killing of Mycobacterium bovis BCG in human alveolar macrophages. Infect Immun. 65(9): p. 3644–7. PMCID: PMC175518. [PubMed: 9284131]
25. Wang CH, Liu CY, Lin HC, Yu CT, Chung KF, and Kuo HP 1998 Increased exhaled nitric oxide in active pulmonary tuberculosis due to inducible NO synthase upregulation in alveolar macrophages. Eur Respir J. 11(4): p. 809–15. [PubMed: 9623681]
26. Haines RJ, Pendleton LC, and Eichler DC 2011 Argininosuccinate synthase: at the center of arginine metabolism. Int J Biochem Mol Biol. 2(1): p. 8–23. PMCID: PMC3074183. [PubMed: 21494411]
27. Skold M and Behar SM 2008 Tuberculosis triggers a tissue-dependent program of differentiation and acquisition of effector functions by circulating monocytes. J Immunol. 181(9): p. 6349–60. [PubMed: 18941226]
28. Erez A, Nagamani SC, Shchelochkov OA, Premkumar MH, Campeau PM, Chen Y, Garg HK, Li L, Mian A, Bertin TK, Black JO, Zeng H, Tang Y, Reddy AK, Summar M, O'Brien WE, Harrison DG, Mitch WE, Marini JC, Aschner JL, Bryan NS, and Lee B 2011 Requirement of argininosuccinate lyase for systemic nitric oxide production. Nat Med. 17(12): p. 1619–26. DOI: 10.1038/nm.2544. PMCID: PMC3348956. [PubMed: 22081021]
29. Patejunas G, Bradley A, Beaudet AL, and O'Brien WE 1994 Generation of a mouse model for citrullinemia by targeted disruption of the argininosuccinate synthetase gene. Somat Cell Mol Genet. 20(1): p. 55–60. [PubMed: 8197477]
30. Perez CJ, Jaubert J, Guenet JL, Barnhart KF, Ross-Inta CM, Quintanilla VC, Aubin I, Brandon JL, Otto NW, DiGiovanni J, Gimenez-Conti I, Giulivi C, Kusewitt DF, Conti CJ, and Benavides F 2010 Two hypomorphic alleles of mouse Ass1 as a new animal model of citrullinemia type I and other hyperammonemic syndromes. Am J Pathol. 177(4): p. 1958–68. DOI: 10.2353/ajpath.2010.100118. PMCID: PMC2947290. [PubMed: 20724589]
31. Sutton VR, Pan YZ, Davis EC, and Craigen WJ 2003 A mouse model of argininosuccinic aciduria: biochemical characterization. Molecular Genetics and Metabolism. 78(1): p. 11–16. [PubMed: 12559843]
32. Guirado E, Rajaram MV, Chawla A, Daigle J, La Perle KM, Arnett E, Turner J, and Schlesinger LS 2018 Deletion of PPARgamma in lung macrophages provides an immunoprotective response against M. tuberculosis infection in mice. Tuberculosis (Edinb). 111: p. 170–177. DOI: 10.1016/j.tube.2018.06.012. [PubMed: 30029904]
33. Joseph C, Quach JM, Walkley CR, Lane SW, Lo Celso C, and Purton LE 2013 Deciphering hematopoietic stem cells in their niches: a critical appraisal of genetic models, lineage tracing, and imaging strategies. Cell Stem Cell. 13(5): p. 520–33. DOI: 10.1016/j.stem.2013.10.010. [PubMed: 24209759]
34. Chennupati R, Meens MJ, Marion V, Janssen BJ, Lamers WH, De Mey JG, and Kohler SE 2014 Endothelial arginine resynthesis contributes to the maintenance of vasomotor function in male

diabetic mice. PLoS One. 9(7): p. e102264 DOI: 10.1371/journal.pone.0102264. PMCID: PMC4102520. [PubMed: 25033204]

35. Hecker M, Sessa WC, Harris HJ, Anggard EE, and Vane JR 1990 The metabolism of L-arginine and its significance for the biosynthesis of endothelium-derived relaxing factor: cultured endothelial cells recycle L-citrulline to L-arginine. Proc Natl Acad Sci U S A. 87(21): p. 8612–6. PMCID: PMC55007. [PubMed: 2236071]
36. Tarasenko TN, Gomez-Rodriguez J, and McGuire PJ 2015 Impaired T cell function in argininosuccinate synthetase deficiency. J Leukoc Biol. 97(2): p. 273–8. DOI: 10.1189/jlb.1AB0714-365R. PMCID: PMC4304424. [PubMed: 25492936]
37. Werner A, Koschke M, Leuchtner N, Luckner-Minden C, Habermeier A, Rupp J, Heinrich C, Conradi R, Closs EI, and Munder M 2017 Reconstitution of T Cell Proliferation under Arginine Limitation: Activated Human T Cells Take Up Citrulline via L-Type Amino Acid Transporter 1 and Use It to Regenerate Arginine after Induction of Argininosuccinate Synthase Expression. Front Immunol. 8: p. 864 DOI: 10.3389/fimmu.2017.00864. PMCID: PMC5523021. [PubMed: 28791021]
38. Rodriguez PC, Quiceno DG, and Ochoa AC 2007 L-arginine availability regulates T-lymphocyte cell-cycle progression. Blood. 109(4): p. 1568–73. DOI: 10.1182/blood-2006-06-031856. PMCID: PMC1794048. [PubMed: 17023580]
39. Kaufmann SH 2001 How can immunology contribute to the control of tuberculosis? Nat Rev Immunol. 1(1): p. 20–30. DOI: 10.1038/35095558. [PubMed: 11905811]
40. Munder M, Schneider H, Luckner C, Giese T, Langhans CD, Fuentes JM, Kropf P, Mueller I, Kolb A, Modolell M, and Ho AD 2006 Suppression of T-cell functions by human granulocyte arginase. Blood. 108(5): p. 1627–34. DOI: 10.1182/blood-2006-11-010389. [PubMed: 16709924]
41. Marakalala MJ, Raju RM, Sharma K, Zhang YJ, Eugenin EA, Prideaux B, Daudelin IB, Chen PY, Booty MG, Kim JH, Eum SY, Via LE, Behar SM, Barry CE, 3rd, Mann M, Dartois V, and Rubin EJ 2016 Inflammatory signaling in human tuberculosis granulomas is spatially organized. Nat Med. 22(5): p. 531–8. DOI: 10.1038/nm.4073. PMCID: PMC4860068. [PubMed: 27043495]
42. Mattila JT, Beaino W, Maiello P, Coleman MT, White AG, Scanga CA, Flynn JL, and Anderson CJ 2017 Positron Emission Tomography Imaging of Macaques with Tuberculosis Identifies Temporal Changes in Granuloma Glucose Metabolism and Integrin alpha4beta1-Expressing Immune Cells. J Immunol. 199(2): p. 806–815. DOI: 10.4049/jimmunol.1700231. PMCID: PMC5520654. [PubMed: 28592427]
43. Davis SL, Nuermberger EL, Um PK, Vidal C, Jedynak B, Pomper MG, Bishai WR, and Jain SK 2009 Noninvasive pulmonary [18F]-2-fluoro-deoxy-D-glucose positron emission tomography correlates with bactericidal activity of tuberculosis drug treatment. Antimicrob Agents Chemother. 53(11): p. 4879–84. DOI: 10.1128/AAC.00789-09. PMCID: PMC2772305. [PubMed: 19738022]
44. Lin PL and Flynn JL 2018 The End of the Binary Era: Revisiting the Spectrum of Tuberculosis. J Immunol. 201(9): p. 2541–2548. DOI: 10.4049/jimmunol.1800993. PMCID: PMC6217958. [PubMed: 30348659]
45. Martinez V, Castilla-Lievre MA, Guillet-Caruba C, Grenier G, Fior R, Desarnaud S, Doucet-Populaire F, and Boue F 2012 (18)F-FDG PET/CT in tuberculosis: an early non-invasive marker of therapeutic response. Int J Tuberc Lung Dis. 16(9): p. 1180–5. DOI: 10.5588/ijtld.12.0010. [PubMed: 22794271]
46. Evans RW, Fernstrom JD, Thompson J, Morris SM, Jr., and Kuller LH 2004 Biochemical responses of healthy subjects during dietary supplementation with L-arginine. J Nutr Biochem. 15(9): p. 534–9. DOI: 10.1016/j.jnutbio.2004.03.005. [PubMed: 15350985]
47. Romero MJ, Platt DH, Caldwell RB, and Caldwell RW 2006 Therapeutic use of citrulline in cardiovascular disease. Cardiovasc Drug Rev. 24(3–4): p. 275–90. DOI: 10.1111/j.1527-3466.2006.00275.x. [PubMed: 17214603]
48. Moinard C, Nicolis I, Neveux N, Darquy S, Benazeth S, and Cynober L 2008 Dose-ranging effects of citrulline administration on plasma amino acids and hormonal patterns in healthy subjects: the Citrudose pharmacokinetic study. Br J Nutr. 99(4): p. 855–62. DOI: 10.1017/S0007114507841110. [PubMed: 17953788]

49. Martinez FO, Gordon S, Locati M, and Mantovani A 2006 Transcriptional profiling of the human monocyte-to-macrophage differentiation and polarization: new molecules and patterns of gene expression. J Immunol. 177(10): p. 7303–11. [PubMed: 17082649]
50. McGuire PJ, Lee HS, C. Members of the Urea Cycle Disorders Consortium, and Summar ML 2013 Infectious precipitants of acute hyperammonemia are associated with indicators of increased morbidity in patients with urea cycle disorders. J Pediatr. 163(6): p. 1705–1710 e1. DOI: 10.1016/j.jpeds.2013.08.029. PMCID: PMC3958925. [PubMed: 24084106]
51. Summar ML, Dobbelaere D, Brusilow S, and Lee B 2008 Diagnosis, symptoms, frequency and mortality of 260 patients with urea cycle disorders from a 21-year, multicentre study of acute hyperammonaemic episodes. Acta Paediatr. 97(10): p. 1420–5. DOI: 10.1111/j.1651-2227.2008.00952.x. PMCID: PMC2675643. [PubMed: 18647279]
52. Morris SM, Jr. 1992 Regulation of enzymes of urea and arginine synthesis. Annu Rev Nutr. 12: p. 81–101. DOI: 10.1146/annurev.nu.12.070192.000501. [PubMed: 1503815]
53. Grimble GK 2007 Adverse gastrointestinal effects of arginine and related amino acids. J Nutr. 137(6 Suppl 2): p. 1693S–1701S. [PubMed: 17513449]
54. Oketch-Rabah HA, Roe AL, Gurley BJ, Griffiths JC, and Giancaspro GI 2016 The Importance of Quality Specifications in Safety Assessments of Amino Acids: The Cases of l-Tryptophan and l-Citrulline. J Nutr. 146(12): p. 2643S–2651S. DOI: 10.3945/jn.115.227280. [PubMed: 27934657]
55. Giannesini B, Le Fur Y, Cozzone PJ, Verleye M, Le Guern ME, and Bendahan D 2011 Citrulline malate supplementation increases muscle efficiency in rat skeletal muscle. Eur J Pharmacol. 667(1–3): p. 100–4. DOI: 10.1016/j.ejphar.2011.05.068. [PubMed: 21664351]
56. Almeida Da Silva PE and Palomino JC 2011 Molecular basis and mechanisms of drug resistance in Mycobacterium tuberculosis: classical and new drugs. J Antimicrob Chemother. 66(7): p. 1417–30. DOI: 10.1093/jac/dkr173. [PubMed: 21558086]

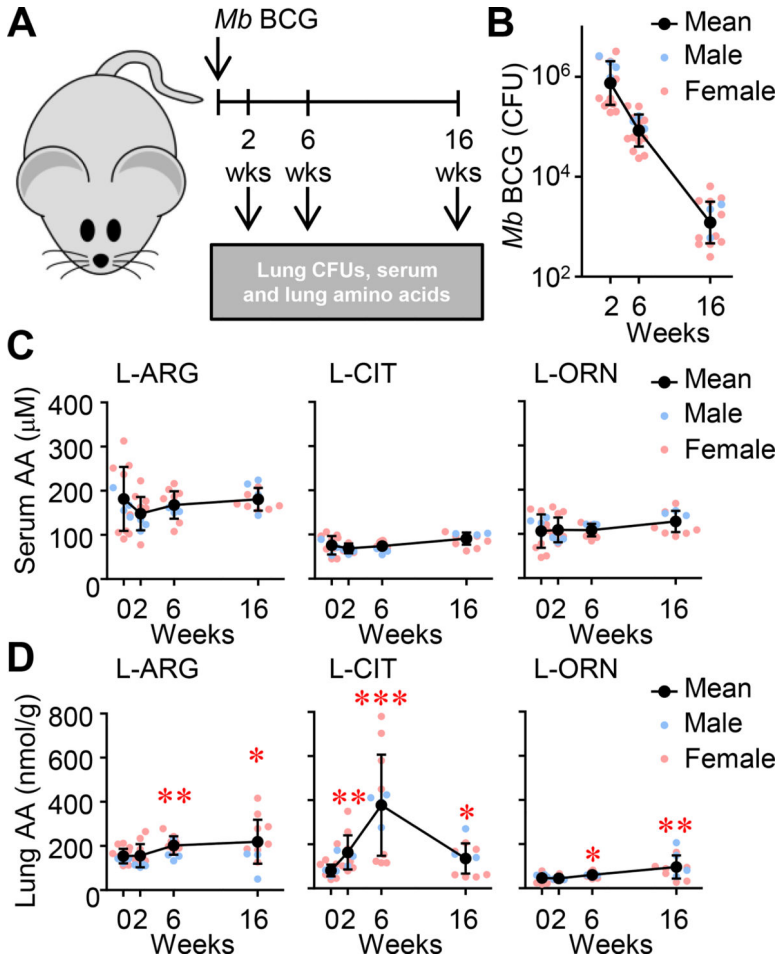

Figure 1. Metabolites of L-ARG metabolism in the lung and serum following pulmonary *M. bovis* BCG infection.

(A) Male and female C57BL/6 mice were infected with *M. bovis* BCG via intranasal inoculation. (B) At 2, 6, and 16 weeks post-infection, CFUs were determined from lung homogenates (N=16, 3 experiments combined). (C, D) Concentrations of L-ARG, L-CIT, and L-ORN in the serum (C) and lung homogenates (relative to lung mass) (D) were determined by LC-MS/MS. (N=12, 2 experiments combined). Data are the individual CFUs or amino acid concentrations (Male = blue, Female = pink), with the mean represented by black symbols. Error bars, SD. *p<0.05, **p<0.01, ***p<0.001 by Student's t test comparing indicated data to uninfected mice (i.e. 0 weeks).

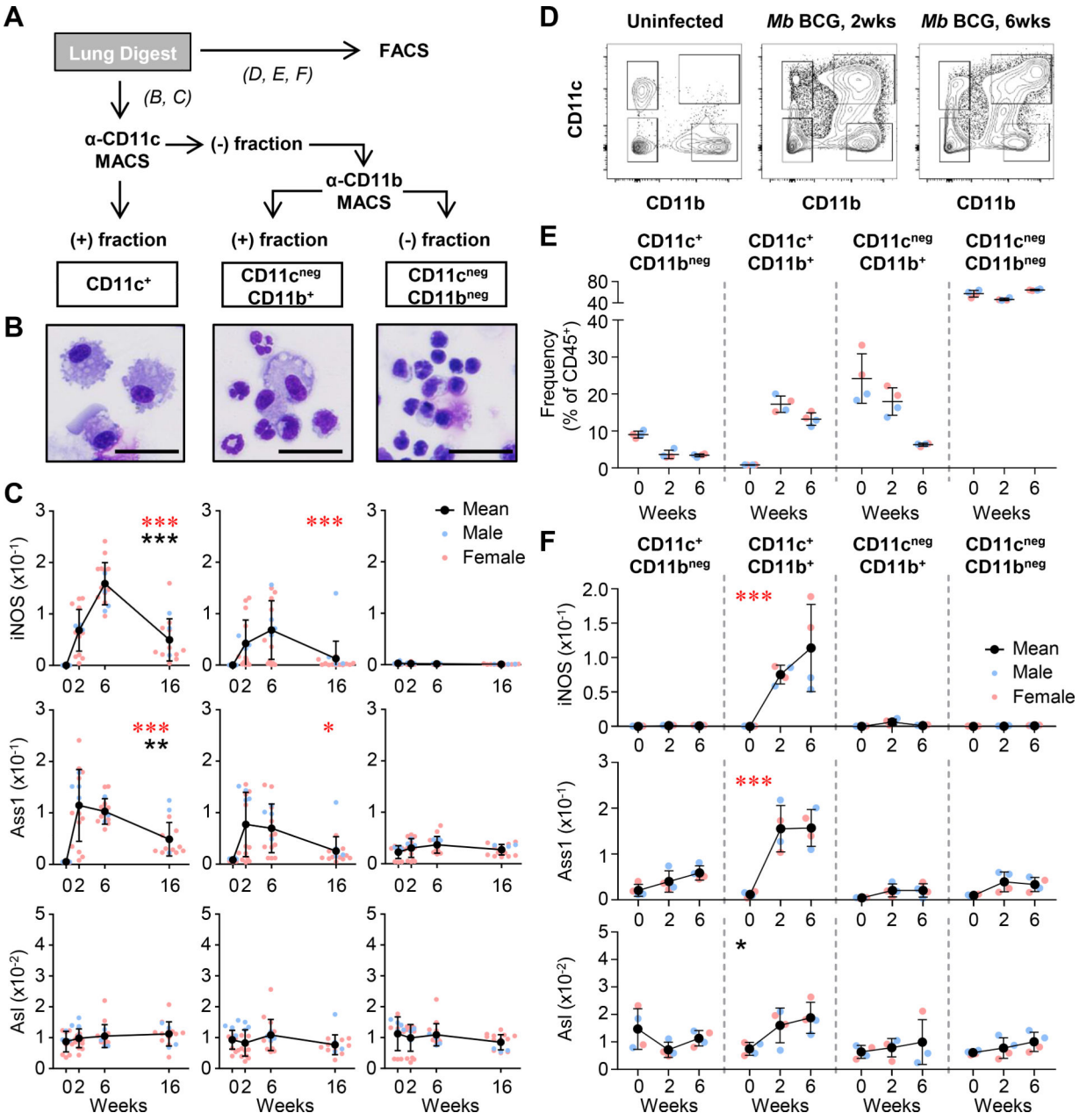

Figure 2. L-ARG synthesis machinery in lung myeloid cells following *M. bovis* BCG infection.

(A) Male and female C57BL/6 mice were infected with *M. bovis* BCG via intranasal inoculation. At 2, 6, and 16 weeks post-infection and from uninfected mice (0 weeks), lung cells were separated by magnetic bead cell sorting (MACS, B and C) or fluorescence activated cell sorting (FACS, D, E, and F). (B) MACS sorted cells were evaluated by microscopy (images shown are from 6 weeks post infection, scale: line = 30 μm). (C) Gene expression analysis from sorted cells by qRT-PCR (N≥11, 3 experiments combined). Data are the individual gene expression values normalized to Gapdh (Male = blue, Female = pink), with the mean represented by black symbols. Error bars, SD. *p<0.05, ***p<0.001 (red) comparing the indicated population to $CD11c^{neg}CD11b^{neg}$ cells by 2-way ANOVA;

**p<0.01, ***p<0.001 (black) comparing $CD11c^{+}$ to $CD11c^{neg}CD11b^{+}$ cells by 2-way ANOVA. (D) Sample flow cytometry histograms from lung digests prior to sorting. (E) Cells from digested lungs were FACS sorted based on expression of CD11c and CD11b, and their relative frequency within hematopoietic cells (i.e. $CD45^{+}$) are shown from uninfected, 2 and 6 weeks post *M. bovis* BCG infection. (F) Gene expression analysis from sorted cells by qRT-PCR (N=4, 1 experiment). Data are the individual gene expression values normalized to Gapdh (each dot represents pooled lung homogenates from 2 mice; Male = blue, Female = pink), with the mean represented by black symbols. Error bars, SD. ***p<0.001 (red) comparing gene expression from $CD11c^{+}CD11b^{+}$ cells to each other population by 2-way ANOVA; *p<0.05 (black) comparing gene expression from $CD11c^{+}CD11b^{+}$ cells to $CD11c^{neg}CD11b^{+}$ and $CD11c^{neg}CD11b^{neg}$ by 2-way ANOVA.

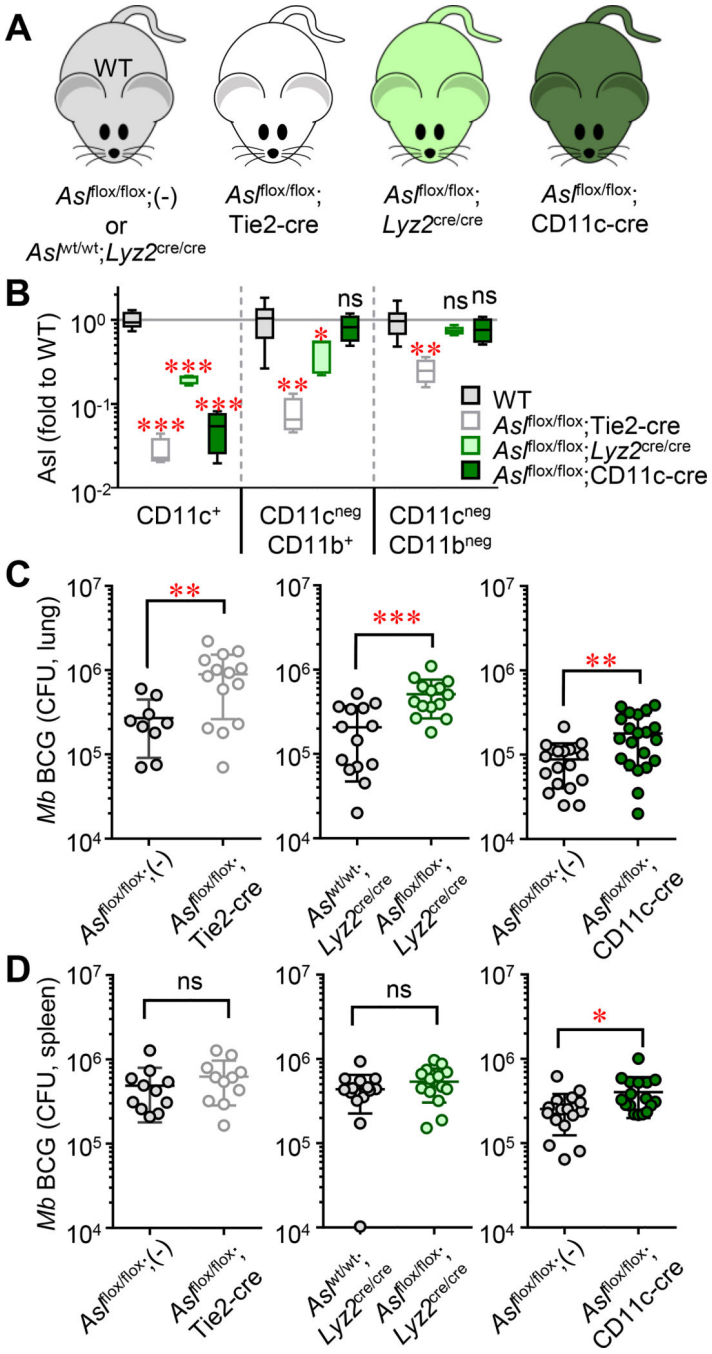

Figure 3. Necessity of myeloid-specific L-ARG synthesis during host defense to *M. bovis* BCG.

(A) Male and female mice were infected with *M. bovis* BCG via intranasal inoculation. Eight weeks post-infection, mice were euthanized and tissues were analyzed by qRT-PCR or CFU enumeration. (B) Deletion of Asl was determined by qRT-PCR in the indicated populations of lung cells separated by MACS as described in Figure 2 (N≥4). Data are presented as box and whisker plots of the normalized Asl expression, relative to WT values in each cell population. (C, D) Lungs (N≥9) and spleens (N≥11) were homogenized and plated for CFUs. Data are presented as a scatter plot of individual CFU values with the line

representing the mean. Error bars, SD. Data are combined from at least two experiments. *p < 0.05, **p < 0.01, ***p < 0.001 by Student's t test.

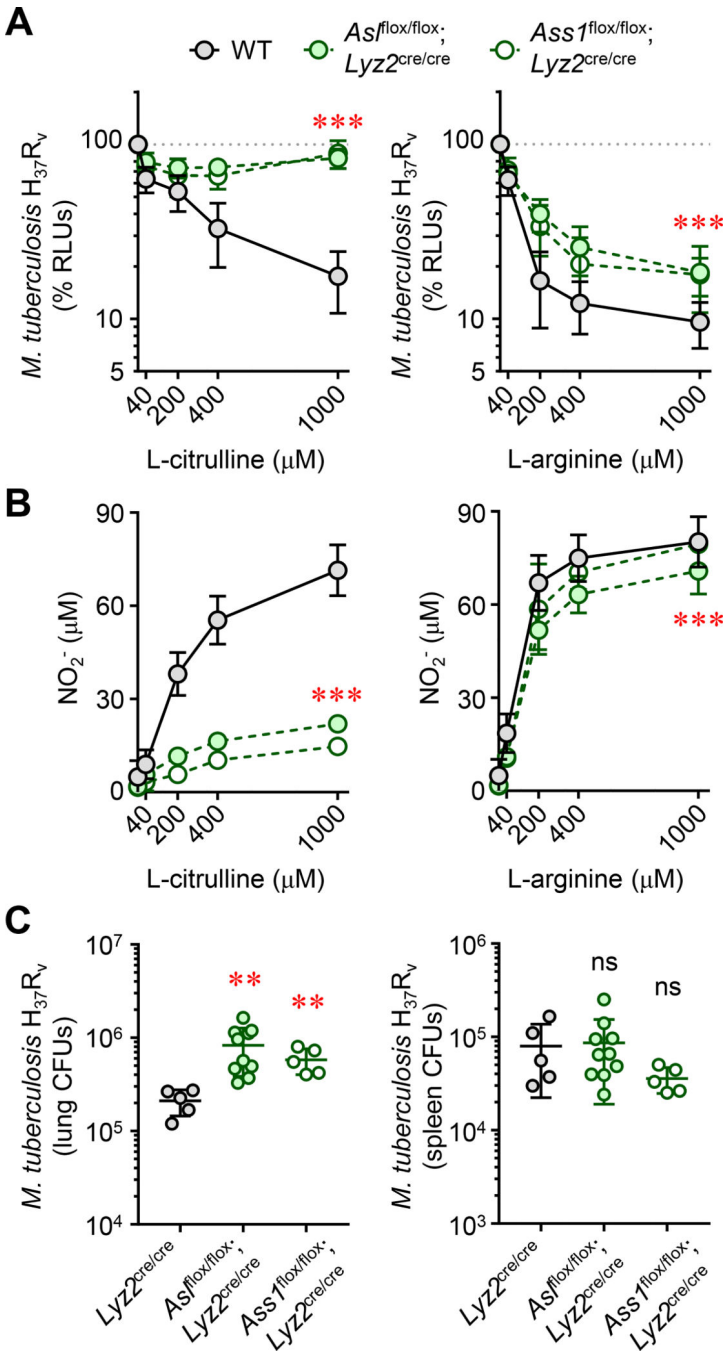

Figure 4. Myeloid-specific L-ARG synthesis is necessary for host defense against virulent *M. tuberculosis*.

(A and B) Thioglycollate-elicited peritoneal-derived macrophages (PDMs) collected from *Asl*$^{flox/flox}$;*Lyz2*$^{cre/cre}$, *Ass1*$^{flox/flox}$;*Lyz2*$^{cre/cre}$, or control mice (N≥8), cultured in titrating L-CIT or L-ARG, were stimulated with IFN-γ and infected with *M. tuberculosis* $H_{37}R_v$. *M. tuberculosis* viability was determined by RLU at 72 hours post-infection (A). Data are the mean percent RLUs (RLUs from cultures without L-CIT or L-ARG were set to 100%). Nitric oxide production was determined by measuring NO_2^- at 72 hours post infection (B). For (A) and (B), the y-axis intersects the x-axis at "0". (C) Male and female

Asl$^{flox/flox}$;*Lyz2*$^{cre/cre}$ (N=10), *Ass1*$^{flox/flox}$;*Lyz2*$^{cre/cre}$ (N=5), or *Lyz2*$^{cre/cre}$ (N=5) control mice were infected with *M. tuberculosis* $H_{37}R_v$ via intranasal inoculation. Eight weeks post-infection, mice were euthanized and the lung and spleen were analyzed by CFU enumeration. Data are presented as a scatter plot of individual CFU values with the line representing the mean. Error bars, SD. Data are combined from at least two experiments (A, B) or are from one of two independent experiments (C). ***$p < 0.001$ comparing either *Asl*$^{flox/flox}$;*Lyz2*$^{cre/cre}$ or *Ass1*$^{flox/flox}$;*Lyz2*$^{cre/cre}$ to WT by 2-way ANOVA (A and B); **$p < 0.01$, comparing indicated data to *Lyz2*$^{cre/cre}$ WT controls by Student's t test (C).table